PHYSICAL REVIEW A **73**, 023806 (2006)

Effect of atomic noise on optical squeezing via polarization self-rotation in a thermal vapor cell

M. T. L. Hsu, G. Hétet, A. Peng, C. C. Harb, H.-A. Bachor, M. T. Johnsson, J. J. Hope, and P. K. Lam*
Australian Centre for Quantum-Atom Optics, Department of Physics, Australian National University, ACT 0200, Australia

A. Dantan, J. Cviklinski, A. Bramati, and M. Pinard
Laboratoire Kastler Brossel, Université Pierre et Marie Curie, case 74, 75252 Paris cedex 05, France
(Received 21 October 2005; published 7 February 2006)

The traversal of an elliptically polarized optical field through a thermal vapor cell can give rise to a rotation of its polarization axis. This process, known as polarization self-rotation (PSR), has been suggested as a mechanism for producing squeezed light at atomic transition wavelengths. We show results of the characterization of PSR in isotopically enhanced rubidium-87 cells, performed in two independent laboratories. We observed that, contrary to earlier work, the presence of atomic noise in the thermal vapor overwhelms the observation of squeezing. We present a theory that contains atomic noise terms and show that a null result in squeezing is consistent with this theory.

DOI: 10.1103/PhysRevA.73.023806 PACS number(s): 42.50.Lc, 42.50.Dv, 42.50.Nn

I. INTRODUCTION

Squeezing is the reduction of the noise variance of an optical field below the quantum noise limit (QNL). Many applications, ranging from increased sensitivity of interferometric measurements [1] to quantum-entanglement-based information protocols [2–4], are reliant on squeezed light. Recently, Duan *et al.* [5] proposed a long-distance quantum communication network that is based on the interaction of atomic ensembles with squeezed and entangled light beams. To achieve such goals, squeezed light at atomic wavelengths is required.

Conventionally, squeezing can be generated via efficient nonlinear optical processes, such as $\chi^{(2)}$ parametric down-conversion [2,6,7]. The transparency windows of nonlinear optical crystals, however, may not coincide with some atomic transitions. For example, commonly used sodium and rubidium atomic transition wavelengths are difficult to access via $\chi^{(2)}$ crystals. Another method of generating squeezed light is to utilize the $\chi^{(3)}$ atomic Kerr effect at the required atomic wavelength. These experiments, however, require ultracold atoms confined in cavities and are therefore technically challenging [8,9].

Recently, there has been a proposal for generating atomic wavelength squeezing via the single traversal of an optical field through a thermal vapor cell [10]. This proposal promises a simple, scalable, and cost-effective means of generating squeezed light for Rb and potentially for other atomic species. Due to the ac Stark shift and optical pumping-induced refractive index changes of the atomic vapor, an elliptically polarized input field will experience an intensity-dependent rotation of the optical polarization axes [11]. This effect, known as polarization self-rotation (PSR), was suggested as a nonlinear mechanism for squeezing [10,12]. Assuming negligible atomic spontaneous emission noise, Matsko *et al.* [10] developed a phenomenological model that treats PSR as a cross-phase modulation mechanism. In the situation of a linearly polarized input field propagating through the vapor cell, a nonlinear cross-phase interaction occurs between the two circularly polarized field components. This results in the squeezing of the output vacuum field mode that is orthogonally polarized to the input field. Analogous to cross-phase modulation squeezing in optical fibres [13–18], it was suggested that 6 dB of PSR squeezing is possible with thermal Rb vapor cells. Subsequently Ries *et al.* [19] reported an observation of 0.85 dB maximum squeezing from a Rb vapor cell and attributed their squeezing to PSR.

The phenomenological model of PSR squeezing by Matsko *et al.* [10] ignored effects such as atomic spontaneous emission. In contrast, Josse *et al.* [20] pointed out the importance of noise terms arising from the atomic dynamics that could possibly degrade, if not totally destroy, squeezing. The model of Josse *et al.* [20] was based on the interaction of a linearly polarized field with four-level atoms. They showed that in the high-saturation regime, the atomic noise contribution could potentially be larger than the squeezing term. Nevertheless, in the low-saturation regime and at sideband frequencies larger than the atomic relaxation rate, squeezing on the vacuum mode can be generated via the cross-Kerr effect induced by the bright field. Such a regime, however, can only be obtained with ultracold trapped atoms enclosed in an optical cavity [9].

This paper is structured as follows: In Sec. II, we review the theoretical works of Matsko *et al.* [10] and Josse *et al.* [20]. We modified the analysis of Josse *et al.* [20] to the case of a single traversal optical field through a thermal vapor cell. In Sec. III, we report measurements of both the transmittivity and the PSR of an elliptically polarized field through an isotopically enhanced ^{87}Rb vapor cell on both the D_1 and D_2 lines. We then study the noise properties of the outgoing vacuum field. The parameter regime investigated extends beyond the squeezing regime reported in Ref. [19]. In contradiction to the results in Ref. [19], no optical squeezing was observed. Instead, we observed excess quadrature noise above the QNL for a wide range of parameters. Finally,

*Electronic address: ping.lam@anu.edu.au

in Sec. IV we relate experimental results to the theory and show that under our experimental conditions, where atomic spontaneous emission is significant, squeezing is overwhelmed by atomic noise terms.

II. THEORY

A. Cross-phase modulation squeezing

For cross-phase modulation squeezing in fibers, a bright input optical pulse in the x polarization is delivered into a weakly birefringent optical fiber. As a result of the $\chi^{(3)}$ nonlinearity in the fiber, the annihilation ($\hat{a}_y$) and creation ($\hat{a}_y^\dagger$) operators for the y polarized vacuum field become coupled [13–16]. The equation of motion for the y-polarized field, in the rotating frame, is given by

$$\frac{\partial}{\partial z}\hat{a}_y(z,t) = i\frac{\kappa}{3}(2|\langle\hat{a}_x\rangle|^2\hat{a}_y + \langle\hat{a}_x\rangle^2\hat{a}_y^\dagger), \tag{1}$$

where $\kappa = n_2\hbar\omega_0^2/(cA)$ is the Kerr coefficient, n_2 is the nonlinear index coefficient of the medium, ω_0 is the carrier frequency, and A is the effective transverse area of the propagating field. The last term of Eq. (1) describes the cross-Kerr coupling between the bright x-and vacuum y-linearly polarized fields, and is responsible for generating squeezing in the y-polarized field.

Matsko *et al.* [10] proposed that the PSR effect in atomic vapor can be used to generate vacuum squeezing. Their proposal was related to the mechanism of cross-phase coupling between two orthogonal polarization fields. We consider the PSR effect [11], where an elliptically polarized field undergoes a rotation in its polarization ellipse upon propagation through an atomic medium. For an optically thin medium, the rotation angle is given by

$$\phi = \mathcal{G}\epsilon(0)l, \tag{2}$$

where $\mathcal{G}$ is the PSR parameter (dependent on the input field intensity and frequency), $\epsilon(0)$ is the input field ellipticity [assumed to be small and constant during propagation, $\epsilon(0) = \epsilon(l)$], and l is the length of the medium. One could take the analogy of the PSR effect to the quantum regime by considering a bright linearly x-polarized input field. The PSR effect projects fluctuations of the bright x-polarized field onto the y-polarized vacuum field. The relative phase between the x- and y-polarized fields then provides amplification or attenuation of the y-polarized field. This effect could potentially result in the reduction of the quantum fluctuations of the y-polarized field.

We will now introduce a methodical representation for our optical field. For a measurement performed in an exposure time T, a freely propagating single-mode optical field can be described by the electric field operator given by

$$\hat{E}(z,t) = \mathcal{E}_0[\hat{a}(z,t)e^{i(kz-\omega t)} + \hat{a}^\dagger(z,t)e^{-i(kz-\omega t)}], \tag{3}$$

where $\mathcal{E}_0 = \sqrt{\hbar\omega/2\epsilon_0 cT\mathcal{A}}$ and $\hat{a}(z,t)$ and $\hat{a}^\dagger(z,t)$ are the slowly varying field envelope annihilation and creation operators, respectively. z is the field propagation axis, ω is the field carrier frequency, and $\mathcal{A}$ is the quantisation cross-section area. We can simplify the expression by introducing $\chi = kz - \omega t$ and phenomenologically extend the classical PSR to the quantum regime. The resulting y-polarized field at the output of the PSR medium is given by

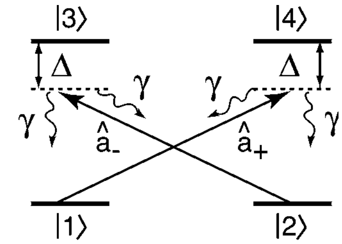

FIG. 1. Two orthogonal σ_+ and σ_- circularly polarized light fields interacting with a four-level atomic system.

$$\hat{E}_y(l) = \mathcal{E}_0[\hat{a}_y(0)(e^{i\chi} - i\mathcal{G}l\cos\chi) + \hat{a}_y^\dagger(0)(e^{-i\chi} + i\mathcal{G}l\cos\chi)]. \tag{4}$$

The noise variance for the $\hat{E}_y(l)$ field, taking into account a phenomenogical absorption parameter α [10], is given by

$$\langle\hat{E}_y^\dagger(l)\hat{E}_y(l)\rangle = \mathcal{E}_0[(1 - 2\mathcal{G}l\sin\chi\cos\chi + \mathcal{G}^2l^2\cos^2\chi)e^{-\alpha l} + (1 - e^{-\alpha l})], \tag{5}$$

where for appropriate values of the phase χ, squeezing of the y-polarized field can be observed. Such a model predicts squeezing values of 6–8 dB below the QNL. However, crucial details such as spontaneous emission and atomic noise are completely ignored, the effects of which can reduce, if not completely destroy, squeezing.

B. Squeezing in a four-level system

Since optical pumping is the main cause of PSR in the high-saturation regime [10,23], which is the relevant regime in our experiment, we can approximate the D_1 and D_2 lines of ^{87}Rb using a four-level atom model. In such a regime, the influence of atomic coherences is negligible. We thus explore the alternative cross-Kerr squeezing model proposed by Josse *et al.* [20]. In the model, four-level atoms interact with two orthogonal circularly polarized fields, as shown in Fig. 1. In the experiment of Ref. [9], squeezing was obtained in the vacuum field (orthogonally polarized to the bright input field) from ultracold trapped atoms, enclosed in a cavity. The four-level squeezing model approximated the level structure of ultracold cesium atoms ($|6S_{1/2}, F=4\rangle$ to $|6P_{3/2}, F=5\rangle$) used in the experiment. In this section, we extend this cavity model to a single-propagation scenario for a single-mode bright x-polarized input field. We derive the equation of motion describing the noise fluctuations of the output y-polarized vacuum field.

The interaction Hamiltonian is given by

$$\hat{\mathcal{H}}_{\text{int}} = \hbar n A_{\text{eff}} \int_0^l dz \{\Delta \hat{\sigma}_{44}(z,t) + \Delta \hat{\sigma}_{33}(z,t) - g[\hat{a}_+(z,t)\hat{\sigma}_{41}(z,t) + \hat{a}_+^\dagger(z,t)\hat{\sigma}_{14}(z,t) + \hat{a}_-(z,t)\hat{\sigma}_{32}(z,t) + \hat{a}_-^\dagger(z,t)\hat{\sigma}_{23}(z,t)]\}, \quad (6)$$

where $\hat{a}_+(z,t)$ and $\hat{a}_-(z,t)$ are the respective slowly varying field envelope operators for the σ_+ and σ_- circularly polarized fields, n is the atomic density, and g is the atom-field coupling constant. The atomic dipole operator at position z in the rotating frame is defined by locally averaging over a transverse slice containing many atoms:

$$\hat{\sigma}_{ij}(z,t) = \frac{1}{nA\,\delta z} \sum_{z_k \in \delta z} e^{i(\omega_i - \omega_j) z_k / c} |i\rangle_k \langle j|_k. \quad (7)$$

The optical Bloch equations for the atomic variables are then given by

$$\frac{\partial}{\partial t}\hat{\sigma}_{14} = -(\gamma + i\Delta)\hat{\sigma}_{14} + ig\hat{a}_+(\hat{\sigma}_{11} - \hat{\sigma}_{44}) + \hat{F}_{14},$$

$$\frac{\partial}{\partial t}\hat{\sigma}_{23} = -(\gamma + i\Delta)\hat{\sigma}_{23} + ig\hat{a}_-(\hat{\sigma}_{22} - \hat{\sigma}_{33}) + \hat{F}_{23},$$

$$\frac{\partial}{\partial t}\hat{\sigma}_{11} = \gamma(\hat{\sigma}_{33} + \hat{\sigma}_{44}) - ig\hat{a}_+\hat{\sigma}_{41} + ig\hat{a}_+^\dagger\hat{\sigma}_{14} + \hat{F}_{11},$$

$$\frac{\partial}{\partial t}\hat{\sigma}_{22} = \gamma(\hat{\sigma}_{33} + \hat{\sigma}_{44}) - ig\hat{a}_-\hat{\sigma}_{32} + ig\hat{a}_-^\dagger\hat{\sigma}_{23} + \hat{F}_{22},$$

$$\frac{\partial}{\partial t}\hat{\sigma}_{33} = -2\gamma\hat{\sigma}_{33} + ig\hat{a}_-\hat{\sigma}_{32} - ig\hat{a}_-^\dagger\hat{\sigma}_{23} + \hat{F}_{33},$$

$$\frac{\partial}{\partial t}\hat{\sigma}_{44} = -2\gamma\hat{\sigma}_{44} + ig\hat{a}_+\hat{\sigma}_{41} - ig\hat{a}_+^\dagger\hat{\sigma}_{14} + \hat{F}_{44}, \quad (8)$$

where we have introduced the spontaneous decay term γ and Langevin noise operators $\hat{F}_{ij}$ that arise from the coupling of atoms to a vacuum reservoir. The Maxwell wave equations describing the σ_+- and σ_--polarized optical fields are given, respectively, by

$$\left(\frac{\partial}{\partial t} + c\frac{\partial}{\partial z}\right)\hat{a}_+(z,t) = igN\hat{\sigma}_{14}(z,t), \quad (9)$$

$$\left(\frac{\partial}{\partial t} + c\frac{\partial}{\partial z}\right)\hat{a}_-(z,t) = igN\hat{\sigma}_{23}(z,t), \quad (10)$$

where N is the total number of atoms. To deduce the noise properties of the field, we linearize the equations around the semiclassical steady state and write the operators in the form $\hat{a} = \langle\hat{a}\rangle + \delta\hat{a}$. Transforming into the Fourier domain and linearizing Eqs. (8)–(10) yields the equation of motion for the quantum fluctuations of the y-polarized vacuum mode $\hat{a}_y = -i(\hat{a}_+ + \hat{a}_-)/\sqrt{2}$, given by

$$\frac{\partial}{\partial \bar{z}}\delta\hat{a}_y = -\Gamma(\omega)\delta\hat{a}_y + \kappa(\omega)(\delta\hat{a}_y - \delta\hat{a}_y^\dagger) + \hat{F}_y, \quad (11)$$

where $\bar{z} = z/l$ and

$$\kappa(\omega) = \kappa(0)\Lambda(\omega),$$

$$\Gamma(\omega) = -i\omega\frac{l}{c} + \kappa(\omega) + \kappa(0)^*\Lambda'(\omega),$$

$$\kappa(0) = \frac{C\gamma}{2(\gamma + i\Delta)}\frac{1}{1+s},$$

$$\Lambda(\omega) = \frac{I_x(\gamma - i\omega)(2\gamma - i\omega)}{2I_x(\gamma - i\omega)^2 - i\omega(2\gamma - i\omega)[(\gamma - i\omega)^2 + \Delta^2]},$$

$$\Lambda'(\omega) = i\omega\frac{I_x(\gamma - i\omega) - (\gamma - i\Delta)(\gamma - i\Delta - i\omega)(2\gamma - i\omega)}{2I_x(\gamma - i\omega)^2 - i\omega(2\gamma - i\omega)[(\gamma - i\omega)^2 + \Delta^2]}, \quad (12)$$

where $C = g^2 Nl/\gamma c$ is the cooperativity parameter, $I_x = |g\langle\hat{a}_x\rangle|^2$ is the mean field intensity, and $s = I_x/(\gamma^2 + \Delta^2)$ is the saturation parameter. The last term of Eq. (11) represents the atomic Langevin noise term and is responsible for a loss or degradation of squeezing. Its exact form and noise spectrum are given and discussed in Sec. IV.

Note that for $\omega = 0$, the imaginary part of $\kappa(0)$ from the second term on the right-hand side of Eq. (11) equates to the first term on the right hand side of Eq. (1). This turns out to be the parameter $\mathcal{G}l$ given in Eq. (2). In the four-level atom model, the PSR for one velocity class increases with the number of atoms and is maximum when $\Delta^2 = \gamma^2 + I_x$. For a Doppler-broadened vapor, $\mathcal{G}l$ can be obtained by summing Eq. (12) over all velocity classes. Note that $\kappa(\omega)$ also gives the amplitude of the cross-Kerr squeezing term in $\delta\hat{a}_y^\dagger$, as in Eq. (11). However, the associated atomic noise contribution must be evaluated in order to obtain the total noise spectrum for the output y-polarized field.

III. EXPERIMENT

In this section, we present experimental results obtained from the two authoring institutions. Both experiments have a similar experimental arrangement. In our experiments, a coherent beam at 795 nm (or 780 nm) was delivered from a Ti:sapphire laser (Coherent MBR-110), as shown in Fig. 2. The laser beam was measured to be quantum noise limited at sideband frequencies $\geqslant 1$ MHz. A small fraction of the beam was sent through another rubidium (Rb) vapor cell for saturated absorption spectroscopy. This provided us with a fine frequency reference for the laser and also allowed the possibility of laser frequency stabilization. The majority of the beam was sent through a polarizer which transmitted the x-polarized field.

In order to measure the PSR and absorption of an input elliptically polarized beam through the vapor cell, the orange-shaded configuration of Fig. 2 was used. The x lin-

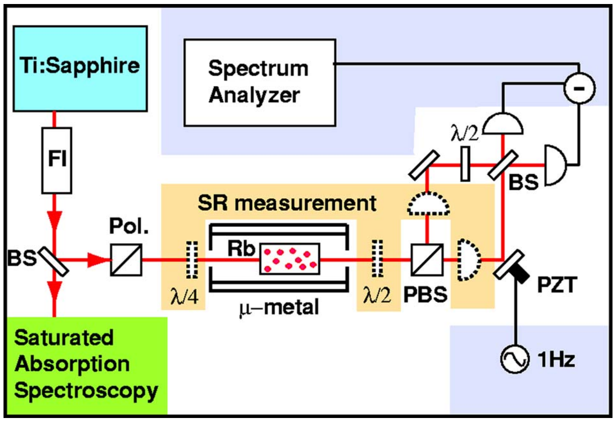

FIG. 2. (Color online) Schematic of the experimental setup. All polarizing optics are of the Glan-Thompson type. FI: Faraday isolator. BS: beam splitter. Pol.: polarizer. PBS: polarizing beam splitter. $\lambda/4$: quarter-wave plate. $\lambda/2$: half-wave plate. PZT: piezoelectric actuator.

early polarized beam was converted into an elliptically polarized beam using a $\lambda/4$-wave plate. The beam (collimated to a waist size of $\sim 425\ \mu$m) then passed through an isotopically enhanced ^{87}Rb vapor cell (75 mm length), which was temperature stabilized at 72 °C (which corresponded to an atomic density of 10^{11} atoms/cm^3). The vapor cell was enclosed in a two-layer μ-metal alloy cylinder, with end caps. The stray magnetic fields within the shielding region were measured to be <2 mG in all three spatial axes. The output beam from the cell was then analyzed using a balanced polarimeter setup, which consisted of a $\lambda/2$-wave plate, a polarizing beam splitter, and two balanced photodetectors. The $\lambda/2$-wave plate was adjusted to balance the powers in the x and y linearly polarized beams from the outputs of the polarizing beam splitter when the frequency of the laser was tuned far off resonance. Thus any rotation of the axis of the input elliptically polarized beam could be measured using the relationship [11]

$$\phi = \frac{V_1 - V_2}{2(V_1 + V_2)}, \qquad (13)$$

where V_1 and V_2 are the dc signals from the photodetectors.

To measure the quadrature noise properties of the y linearly polarized vacuum beam, we then performed homodyne detection, as shown in Fig. 2, using the x linearly polarized output of the polarizing beam splitter as a local oscillator.

A. Classical results

The PSR and transmission of an input elliptically polarized beam through the Rb vapor cell were measured by scanning the laser frequency across the energy levels of interest for a fixed input beam intensity. For the D_2 line, the relevant levels were $|5^2S_{1/2},F_g{=}2\rangle$ to $|5^2P_{3/2},F_e{=}1,2,3\rangle$ and, for the D_1 line, $|5^2S_{1/2},F_g{=}2\rangle$ to $|5^2P_{1/2},F_e{=}1,2\rangle$. We repeated the measurement for varying input beam powers and obtained a contour map of PSR and transmission as a function of laser frequency detuning and input beam intensity, shown in Figs. 3, 4, 6, and 7.

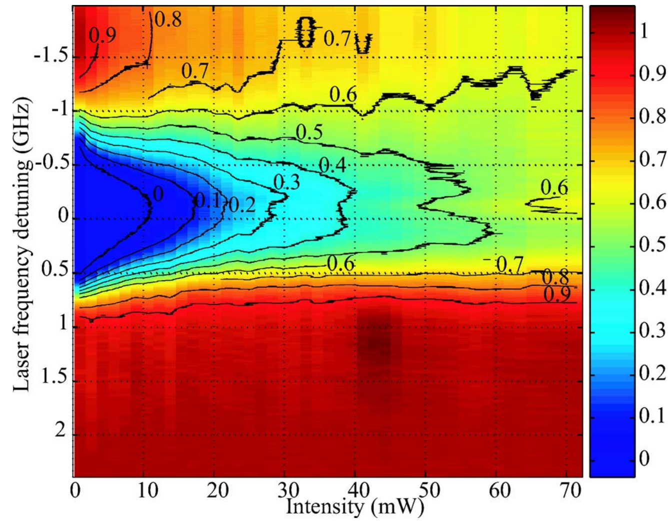

FIG. 3. (Color online) False color contour plot of the normalized transmission results for the D_2 line as a function of input beam intensity and laser frequency detuning. Zero frequency corresponds to the $|5^2S_{1/2},F_g{=}2\rangle$ to $|5^2P_{3/2},F_e{=}3\rangle$ energy levels.

The transmission results for the D_2 line are shown in Fig. 3. The region of lowest transmission, <10%, occurred at input beam intensities $\leqslant$15 mW, around laser frequencies close to zero detuning. For input beam powers $\geqslant$30 mW greater transmission ($\geqslant$30%) was observed. However, power broadening effects were also observed for higher input beam powers, with reduced transmission at frequencies $\leqslant -1$ GHz. The transmission was nonsymmetric with high transmission (>90%) for frequencies $\geqslant$1 GHz, while reduced transmission (>60%) for frequencies $\leqslant -1$ GHz. This was due to the level structure of the excited states of the D_2 line, where the separations between the hyperfine levels are small (within a frequency band of $\sim$0.5 GHz). Power broadening effects were also observed for input beam intensities $\geqslant$30 mW.

The PSR results for the D_2 line are shown in Fig. 4. The regions of largest PSR were 0.3 GHz and −0.6 GHz. The input beam powers which gave the largest $\mathcal{G}l$ magnitudes of 8 and 13 were $\sim$8 mW and $\sim$30 mW, respectively. Zero $\mathcal{G}l$ around zero detuning for input beam powers $\leqslant$15 mW was due to the low transmission of the input beam for the optically thick ^{87}Rb vapor cloud. However, at frequency detunings $\geqslant$0.5 and $\leqslant -0.5$ GHz, significant PSR was observed even though the transmission was reduced. For input beam intensities $\geqslant$20 mW, the PSR was preferentially larger with positive-frequency detunings as opposed to negative-frequency detunings.

In order to explain the asymmetry present in the PSR results, we modeled the hyperfine energy levels of the D_2 line and took into account Doppler broadening. The theoretical fits to the experimental data are shown in Fig. 5.

The reduction in PSR in the negative-frequency detuning region was due to reduced transmission, as observed in Fig. 3. Broadening of the PSR profile was observed for higher input beam powers.

The transmission results for the D_1 line are shown in Fig. 6. The region of lowest transmission (<50%) occurred for

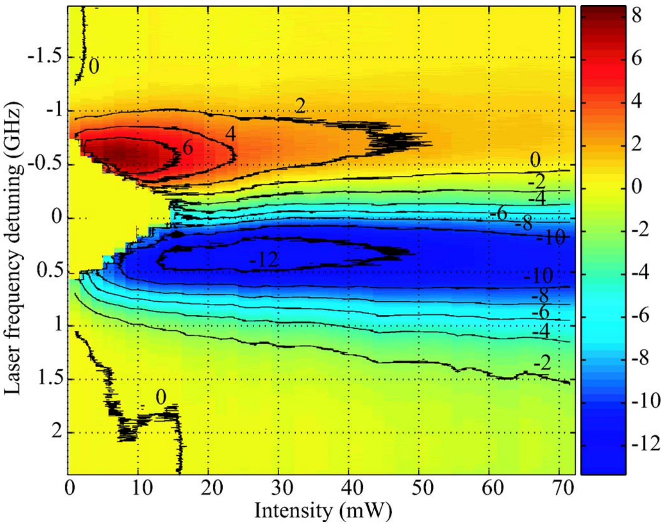

FIG. 4. (Color online) False color contour plot of $\mathcal{G}l$ for the D_2 line, normalized to the input beam ellipticity of 2°, as a function of input beam intensity and laser frequency detuning. Zero frequency corresponds to the $|5^2S_{1/2},F_g=2\rangle$ to $|5^2P_{3/2},F_e=3\rangle$ energy levels.

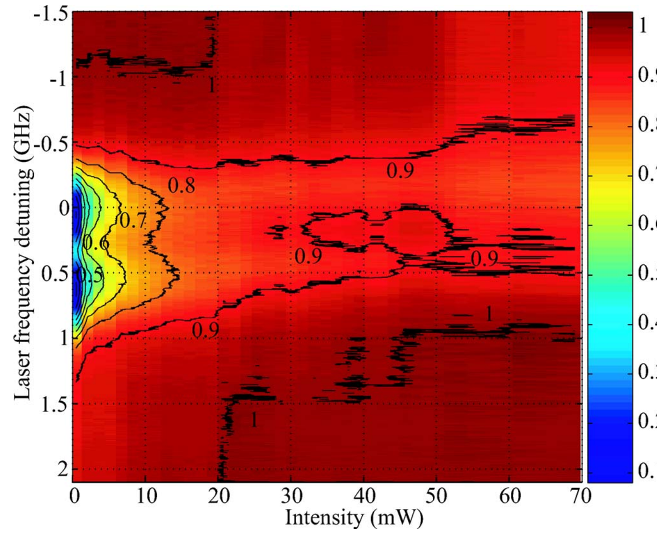

FIG. 6. (Color online) False color contour plot of the normalized transmission results for the D_1 line, as a function of input beam intensity and laser frequency detuning. Zero frequency corresponds to the $|5^2S_{1/2},F_g=2\rangle$ to $|5^2P_{1/2},F_e=1\rangle$ energy levels.

input beam intensities ≤3 mW. These regions were confined around two frequency detuning bands, the −0.2–0.25-GHz band and the 0.4–0.8-GHz band. The two frequency bands corresponded to the absorption lines centered at the $|5^2S_{1/2},F_g=2\rangle$ to $|5^2P_{1/2},F_e=1\rangle$ and $|5^2S_{1/2},F_g=2\rangle$ to $|5^2P_{1/2},F_e=2\rangle$ energy levels, respectively. For input beam powers ≥5 mW, significant transmission was observed (>70%). For most input beam powers, the transmission of the D_1 line was significantly higher than that of the D_2 line. This was due to the weaker atom-field coupling in the D_1 line compared to the D_2 line.

The PSR results for the D_1 line are shown in Fig. 7. The regions of largest PSR occurred at frequency detunings −0.15 GHz and 0.6 GHz. The input beam powers that gave the largest $\mathcal{G}l$ magnitudes of 10 and 11 were ~35 mW and ~22 mW, respectively. Significant PSR was observed for input beam powers >3 mW since the transmission was always >50%. The $\mathcal{G}l$ magnitude was almost equal in both frequency bands corresponding to the two absorption lines centered at the $|5^2S_{1/2},F_g=2\rangle$ to $|5^2P_{1/2},F_e=1\rangle$ and $|5^2S_{1/2},F_g=2\rangle$ to $|5^2P_{1/2},F_e=2\rangle$ energy levels for most input beam powers. This was due to the excited-state level structure of the D_1 line, where the two excited-state levels have a large separation of ~0.8 GHz. This is illustrated by modeling the hyperfine excited-state level structure of the D_1 line. The theoretical fits to the experimental data are shown in Fig. 8.

The two transmission dips are of approximately the same magnitude, resulting in the two PSR peaks being of equal magnitudes.

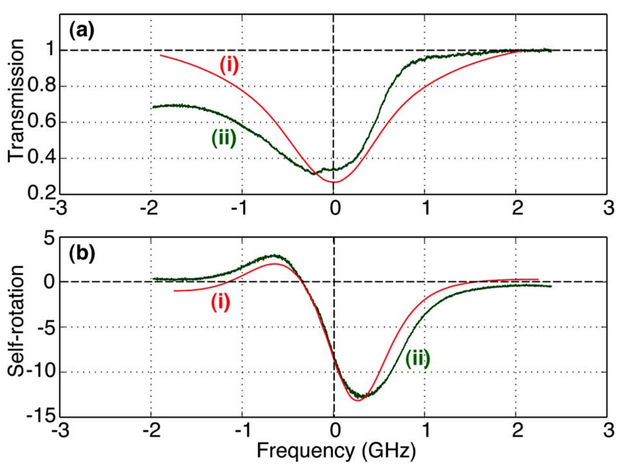

FIG. 5. (Color online) The normalized transmission and $\mathcal{G}l$ results for the D_2 line are shown in (a) and (b), respectively. The (i) red curves are the theoretical fits to the experimental results [(ii) green curve]. Input beam intensity=31.5 mW, and zero frequency corresponds to the $|5^2S_{1/2},F_g=2\rangle$ to $|5^2P_{3/2},F_e=3\rangle$ energy levels.

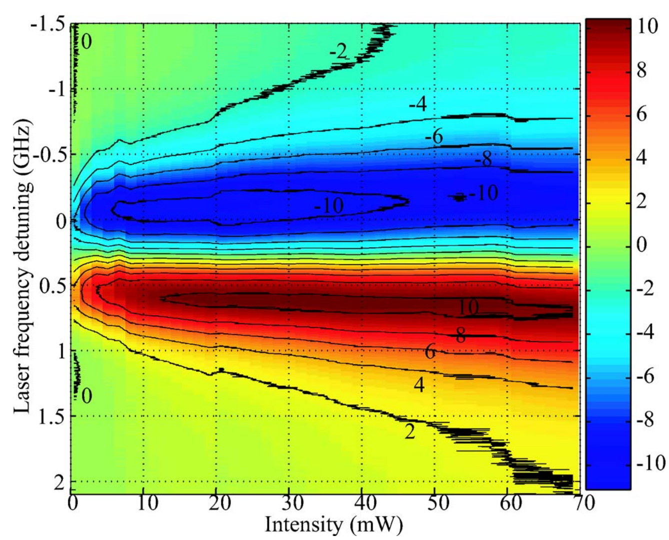

FIG. 7. (Color online) False color contour plot of $\mathcal{G}l$ for the D_1 line, normalized to the input beam ellipticity of 2°, as a function of input beam intensity and laser frequency detuning. Zero frequency corresponds to the $|5^2S_{1/2},F_g=2\rangle$ to $|5^2P_{1/2},F_e=1\rangle$ energy levels.

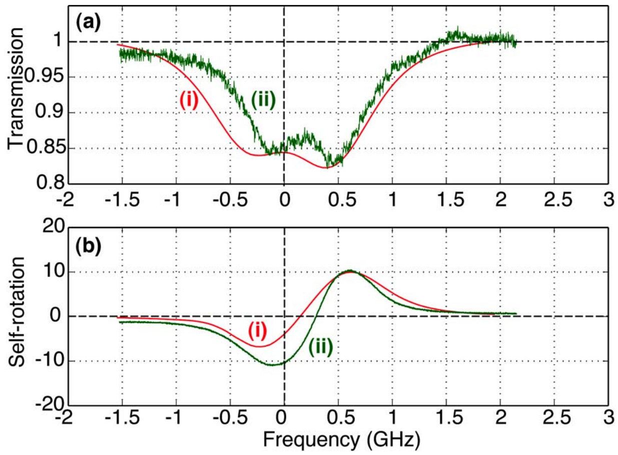

FIG. 8. (Color online) The normalized transmission and $\mathcal{G}l$ results for the D_1 line are shown in (a) and (b), respectively. The (i) red curves are the theoretical fits to the experimental results [(ii) green curve]. Input beam intensity=22.3 mW, and zero frequency corresponds to the $|5^2S_{1/2},F_g=2\rangle$ to $|5^2P_{1/2},F_e=1\rangle$ energy levels.

B. Quantum results

The input field was linearly polarized in the x axis, and we measured the quadrature noise of the outgoing y-polarized vacuum field using the homodyne detection setup shown in Fig. 2. The bright x-polarized output field was used as a local oscillator. The fringe visibility of the interferometer was 99%. The two outputs of the interferometer were then detected using two balanced silicon photodetectors (which consisted of Hamamatsu S3883 photodiodes with measured quantum efficiency values of 94.6%) with bandwidths of ~20 MHz. Blocking the weak field provided a measurement of the QNL. The QNL was checked for linearity with beam power, and the common mode rejection was optimized to ~30–40 dB from 100 kHz to 10 MHz. We also checked that the polarizing beam splitter was well aligned such that negligible amounts of the x-polarized field emerged at the y-polarized output port. The results of the noise measurement for various sideband frequencies at various laser frequency detunings and input beam powers are shown in Figs. 9 (D_2 line) and 11 (D_1 line).

The largest quadrature noise observed for the D_2 line was 10 dB at a detuning of −70 MHz as shown in Fig. 9(c). A time-scanned quadrature noise measurement is shown in Fig. 10.

In the noise plots of Figs. 9(a), 9(c), and 9(d), we observed large levels of excess noise of typically 5 dB above the QNL. In Fig. 9(b) the excess noise level was 0.8 dB above the QNL. This was the lowest noise level observed around zero detuning. The largest values of the phase quadrature noise level corresponded to the regions of maximum PSR as shown in Fig. 4. At large frequency detunings from resonance, both quadrature noise levels were reduced to the QNL.

The noise measurements of the output vacuum field, for the D_1 line, are shown in Fig. 11.

The largest noise modulation observed was 7 dB which occurred at a frequency detuning of 150 MHz as shown in Fig. 11(c). In Figs. 11(a)–11(d), the phase quadrature noise level around zero detuning was always above the QNL due to the presence of large excess noise (3–4 dB). The largest values of the amplitude noise level corresponded to the regions of maximum PSR as shown in Fig. 7. At large frequency detunings from resonance, both quadrature noise levels were reduced to the QNL.

The noise measurement results presented do not vary qualitatively with varying beam focussing geometry, incident power, or temperature. A large amount of excess noise was systematically observed close to resonance. We also per-

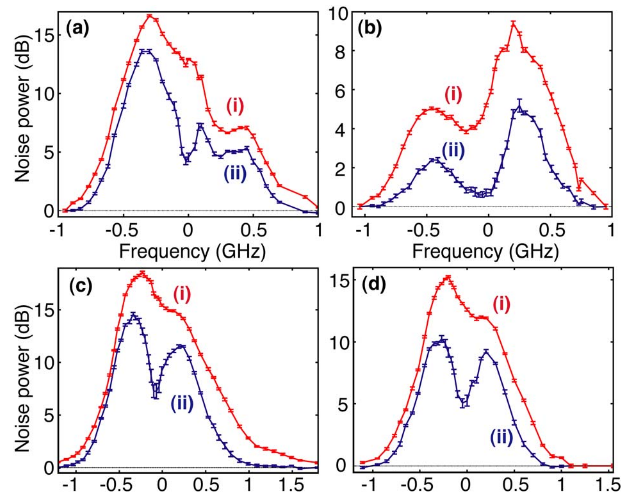

FIG. 9. (Color online) (i) Amplitude and (ii) phase quadrature noise results for the D_2 line, normalized to the QNL and dark noise subtracted. (a) and (b) correspond to an input beam power of 21 mW at sideband frequencies of 3 MHz and 6 MHz, respectively. (c) and (d) are results for an input beam power of 35 mW at sideband frequencies of 3 MHz and 6 MHz, respectively. Zero frequency corresponds to the $|5^2S_{1/2},F_g=2\rangle$ to $|5^2P_{3/2},F_e=3\rangle$ energy level. ResBW: 100 kHz. VBW: 30 Hz.

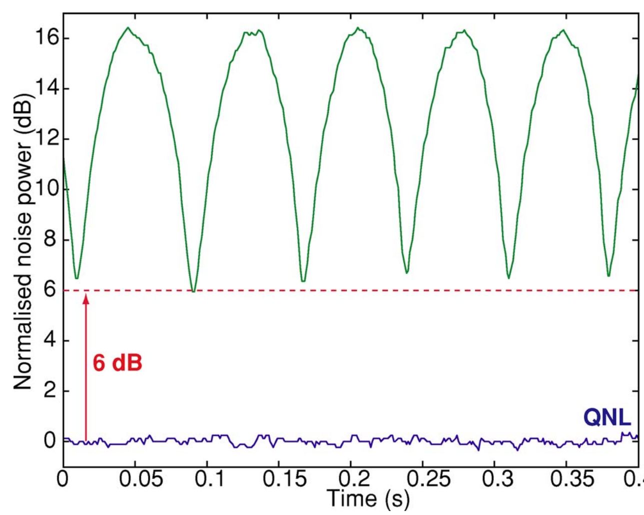

FIG. 10. (Color online) Scanned quadrature noise for the D_2 line measured in zero span at a sideband frequency of 3 MHz. The input beam power was 35 mW, and the laser frequency was −70 MHz from the $|5^2S_{1/2},F_g=2\rangle$ to $|5^2P_{1/2},F_e=3\rangle$ energy level. All plots are dark noise subtracted. ResBW: 100 kHz. VBW: 30 Hz.

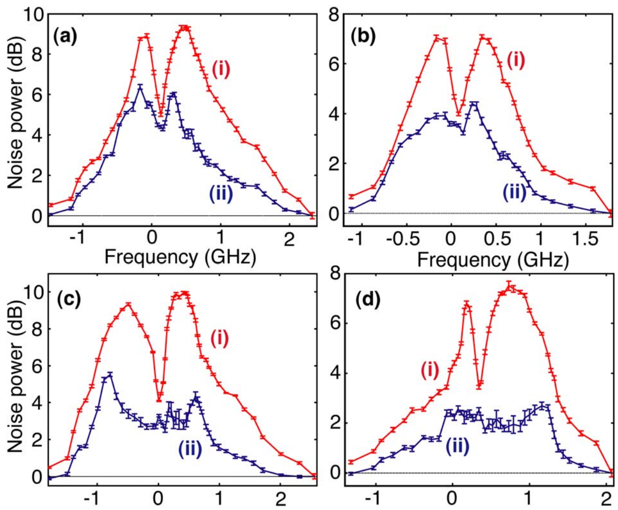

FIG. 11. (Color online) (i) Amplitude and (ii) phase quadrature noise results for the D_1 line, normalized to the QNL and subtracted by the dark noise. (a) and (b) correspond to an input beam power of 21 mW at sideband frequencies of 3 MHz and 6 MHz, respectively. (c) and (d) are results for an input beam power of 35 mW at sideband frequencies of 3 MHz and 6 MHz, respectively. Zero frequency corresponds to the $|5^2S_{1/2},F_g=2\rangle$ to $|5^2P_{1/2},F_e=1\rangle$ energy level. ResBW: 100 kHz. VBW: 30 Hz.

formed similar experiments using paraffin-coated cells and cells containing buffer gas, none of which resulted in the observation of squeezing. Although the PSR and transmission results measured were in a very similar regime to that of Ref. [19], the quantum noise results are not in agreement with either the predictions of Ref. [10] or the observations of Ref. [19]. We use the model presented in Sec. II B to discuss our experimental observations.

IV. DISCUSSION AND CONCLUSIONS

A. Langevin noise analysis

In order to contrast the effect of the atomic noise terms with the squeezing term in Eq. (11), we consider the Langevin term given by

$$\hat{F}_y = \frac{gNl}{c}\left[(A+B)\hat{f}_y + B\hat{f}_y^\dagger + i\sqrt{I_x}A\left(\frac{\hat{f}_z}{-i\omega} + \frac{\hat{f}_z'}{2\gamma - i\omega}\right)\right], \tag{14}$$

where

$$A = \frac{(\gamma - i\Delta - i\omega)(-i\omega)(2\gamma - i\omega)}{D},$$

$$B = \frac{I_x(\gamma - i\omega)}{D},$$

$$D = 2I_x(\gamma - i\omega)^2 - i\omega(2\gamma - i\omega)[(\gamma - i\omega)^2 + \Delta^2],$$

with $I_x = |g\langle\hat{a}_x\rangle|^2$, $\hat{f}_y = (\hat{F}_{14} + \hat{F}_{23})/\sqrt{2}$, $\hat{f}_z = (\hat{F}_{22} - \hat{F}_{11})/\sqrt{2}$, and $\hat{f}_z' = (\hat{F}_{44} - \hat{F}_{33})/\sqrt{2}$. The contribution of this noise term, which depends on the sideband frequency, is to be compared with the cross-Kerr squeezing term $\kappa(\omega)$. As shown in Ref. [20], in the low-saturation regime, large excess atomic noise associated with optical pumping on the y-polarized field dominates at sideband frequencies *lower* than the spontaneous emission rate ($\omega \ll \gamma$). In the low-sideband-frequency regime (assuming $\Delta \gg \gamma$), one obtains

$$\frac{\partial}{\partial z}\delta\hat{a}_y = i\frac{\delta_0}{1+s}\delta\hat{a}_y^\dagger + \frac{gNl}{2\gamma c}\left(\hat{f}_y + \hat{f}_y^\dagger + \frac{\Delta}{2\sqrt{I_x}}\hat{f}_z\right), \tag{15}$$

where $\delta_0 = C\gamma/2\Delta$ denotes the linear dephasing. Ignoring depletion of the mean x-polarized field, the Langevin noise contribution is shown to be proportional to C/gl at least. For the experiment, this quantity is greater than the QNL, such that large excess noise is present in all quadratures for low sideband frequencies, even when absorption is ignored. One therefore cannot observe squeezing in this regime.

In the experiment, the quantum noise of the vacuum field was measured only for sideband frequencies *greater* than the excited-state decay rate ($\omega \gg \gamma$). In this high-sideband-frequency regime (assuming $\Delta \gg \gamma$), we obtain succinct expressions for $\kappa(\omega)$, $\Gamma(\omega)$, and $\tilde{F}_y$ given by

$$\kappa(\omega) = \frac{-i\delta_0 s}{(1+s)(1+2s)}, \quad \Gamma(\omega) = \frac{-i\delta_0}{1+s}, \tag{16}$$

$$\hat{F}_y \simeq -i\frac{gNl}{\Delta c(1+2s)}[(1 + I_x/\omega\Delta)\hat{f}_y + (I_x/\omega\Delta)\hat{f}_y^\dagger - (\sqrt{I_x}/\omega)(\hat{f}_z + \hat{f}_z')]. \tag{17}$$

The above equations describe the atomic noise contribution that may degrade the squeezing of the output y-polarized vacuum field.

The optimization of squeezing is dependent on finding a regime that has low absorption and strong nonlinearity. We now proceed by dividing the discussion into low- and high-atomic-transition-saturation regimes.

B. Low-saturation regime with ultracold atoms

Since cold atoms have higher atomic density, one can operate in the low-saturation regime ($s \ll 1$) and still obtain strong PSR with minimal atomic noise [9] when off resonance. In the Kerr limit ($\Delta \gg \sqrt{I_x} \gg \gamma$), the equation of motion for the vacuum field fluctuations is given by

$$\frac{\partial}{\partial z}\delta\hat{a}_y = i\delta_0\delta\hat{a}_y - i\delta_0 s(2\delta\hat{a}_y - \delta\hat{a}_y^\dagger) - i\frac{gNl}{c\Delta}\hat{f}_y. \tag{18}$$

One recovers in the equation above the same terms as in the cavity model of Ref. [20] under the same approximations. The term in $\delta_0\delta\hat{a}_y$ corresponds to the linear dephasing, the second term gives the cross-Kerr squeezing term, and the Langevin noise contribution corresponding to the last term can be shown to be proportional to $C\gamma^2/\Delta^2$, which can be small in the off-resonant situation ($\Delta \gg \gamma$). In accordance with the prediction of Ref. [20] and the experimental observations of Ref. [9] vacuum squeezing can be generated when $\delta_0 s \sim 1$ and $C\gamma^2/\Delta^2$.

C. High-saturation regime with thermal vapor cell

Contrary to the situation of cold atoms, the Doppler broadening in a thermal vapor makes it impossible to work in the low-saturation regime while simultaneously having low absorption or high nonlinearity. It is however possible to observe strong PSR in the high-saturation regime. In this regime, the atomic noise term is significantly different to that given in Eq. (18). For $I_x \gg \Delta^2$, the equation of motion is given by

$$\frac{\partial}{\partial \overline{z}} \delta \hat{a}_y = \frac{i\delta_0}{2s}(\delta \hat{a}_y + \delta \hat{a}_y^{\dagger}) - i\frac{gNl}{c\omega}(\hat{f}_y + \hat{f}_y^{\dagger}). \qquad (19)$$

As we have seen experimentally with the PSR measurements, the nonlinear term in $\delta_0/(2s) = \mathcal{G}l$ can still be significant when the number of atoms is increased. However, the optical pumping processes associated with PSR now produce a lot of excess noise even in the high-sideband-frequency regime. The contribution of the last term in Eq. (19) can be shown to be proportional to $C\gamma^2/\omega^2 \gg 1$. For our experimental parameters, the atomic noise prevents the observation of squeezing at all sideband frequencies.

D. Further considerations

We now discuss the possible discrepancies between the theoretical models and the experiment. Due to the complexity of the problem, many effects have not been taken into account in the various models discussed in this paper.

First, the presence of resonance fluorescence has not been considered in Ref. [10]. In Ref. [20], it was shown that PSR cannot generate squeezing in the low-saturation regime because of optical pumping processes. We have shown in this paper that this is also true in the high-saturation regime where the resonance fluorescence noise dominates over the cross-Kerr squeezing term *even* at high detection frequencies. This conclusion is in agreement with other observations [21–23].

Second, none of the models presented have included the Doppler effect. Since we are dealing with thermal atoms, the passage of light through the atoms will give rise to a range of observed atomic detuning. The integrated effect due to Doppler broadening will be detrimental to the observation of squeezing.

Third, the multilevel hyperfine structure of the excited states of ^{87}Rb has only been considered for theoretical fits to the classical PSR results, but have not been included in any of the squeezing models. The experimental PSR data presented in this paper clearly show that the multilevel hyperfine structure causes observable asymmetry in the PSR spectrum. This feature cannot be explained by any of the theoretical models presented in Sec. II. The multilevel theory can be expanded to include Langevin noise terms. However, a simple four-level atom model is sufficient to demonstrate the lack of squeezing. The multilevel structure is also certainly less favorable to the generation of squeezing when compared with a simplified four-level model. Different hyperfine levels will not contribute constructively towards a collective interaction that will generate squeezing. The added noise from these different levels will add up significantly. The inclusion of Doppler broadening and multilevel effects would only result in a dominance of the atomic noise term over the squeezing term.

Finally, the propagation of the transverse intensity profile of the input field has been totally ignored in all models. A full treatment of the process should include the multimodal analysis of the evolution of the transverse field modes during propagation through the vapor cell. In the high-saturation regime and for high atomic densities, self-focusing is readily observed. This is due to the atom induced Kerr-lens effect on the optical field. Thus the center of the field intensity distribution will undergo greater PSR than the edges. The cross-Kerr nonlinearity and the atomic absorption used in our calculations are a result of an "integrated" effect of the various transverse modes. It therefore does not model accurately the situation of the experiment. Similar to the previous argument, it is unlikely that the multimodal consideration of the process will yield better squeezing.

E. CONCLUSION

We have presented experimental results of PSR from two independent laboratories and have observed no squeezing. Instead we have observed excess noise in the output field spectrum at all sideband frequencies. We have modeled semiclassically the multilevel hyperfine structure of ^{87}Rb and obtained theoretical fits to the experimental PSR data. Our multilevel modeling can predict the asymmetry in the PSR, which is due to the presence of other hyperfine excited states. We considered a quantum-mechanical four-level atomic model and showed that the squeezing term is overwhelmed by atomic noise terms in the situation of a thermal vapor. The effects of resonance fluorescence, the Doppler effect, and the multilevel hyperfine structure of ^{87}Rb all contribute to overwhelm the squeezing term. Therefore, it is expected that a full quantum-mechanical treatment of a multilevel ^{87}Rb atom will yield a result where squeezing cannot be generated. In spite of this, the four-level atom model shows that squeezing can be generated in the situation of cold atoms where the Doppler effect is negligible. When the input field is off resonance, the nonlinearity is large but the absorption low, such that the atomic noise term does not overwhelm the squeezing term.

ACKNOWLEDGMENTS

We would like to thank P. Drummond, W. P. Bowen, J. J. Longdell, and A. I. Lvovsky for fruitful discussions and Paul Tant for technical support. This research was funded under the Australian Research Council Centre of Excellence Programme and the European Project No. FP6-511004 (COVAQIAL).

[1] K. McKenzie, D. A. Shaddock, D. E. McClelland, B. C. Buchler, and P. K. Lam, Phys. Rev. Lett. **88**, 231102 (2002).
[2] Z. Y. Ou, S. F. Pereira, H. J. Kimble, and K. C. Peng, Phys. Rev. Lett. **68**, 3663 (1992).
[3] A. Furusawa, J. L. Sorensen, S. L. Braunstein, C. A. Fuchs, H. J. Kimble, and E. S. Polzik, Science **282**, 706 (1998).
[4] W. P. Bowen, N. Treps, B. C. Buchler, R. Schnabel, T. C. Ralph, Hans-A. Bachor, T. Symul, and P. K. Lam, Phys. Rev. A **67**, 032302 (2003).
[5] L.-M. Duan, M. D. Lukin, J. I. Cirac, and P. Zoller, Nature (London) **414**, 413 (2001).
[6] P. K. Lam, T. C. Ralph, B. C. Buchler, D. E. McClelland, H.-A. Bachor, and J. Gao, J. Opt. B: Quantum Semiclassical Opt. **1**, 469 (1999).
[7] J. L. Sorensen, J. Hald, and E. S. Polzik, Phys. Rev. Lett. **80**, 3487 (1998).
[8] A. Lambrecht, T. Coudreau, A. M. Steinberg, and E. Giacobino, Europhys. Lett. **36**, 93 (1996).
[9] V. Josse, A. Dantan, L. Vernac, A. Bramati, M. Pinard, and E. Giacobino, Phys. Rev. Lett. **91**, 103601 (2003).
[10] A. B. Matsko, I. Novikova, G. R. Welch, D. Budker, D. F. Kimball, and S. M. Rochester, Phys. Rev. A **66**, 043815 (2002).
[11] S. M. Rochester, D. S. Hsiung, D. Budker, R. Y. Chiao, D. F. Kimball, and V. V. Yashchuk, Phys. Rev. A **63**, 043814 (2001).
[12] I. Novikova, A. B. Matsko, and G. R. Welch, J. Mod. Opt. **49**, 2565 (2002).
[13] L. Boivin and H. A. Haus, Opt. Lett. **21**, 146 (1996).
[14] M. Margalit, C. X. Yu, E. P. Ippen, and H. A. Haus, Opt. Express **2**, 72 (1998).
[15] K. Bergman and H. A. Haus, Opt. Lett. **16**, 663 (1991).
[16] K. Bergman, C. R. Doerr, H. A. Haus, and M. Shirasaki, Opt. Lett. **18**, 643 (1993).
[17] M. Rosenbluh and R. M. Shelby, Phys. Rev. Lett. **66**, 153 (1991).
[18] Ch. Silberhorn, P. K. Lam, O. Weiss, F. König, N. Korolkova, and G. Leuchs, Phys. Rev. Lett. **86**, 4267 (2001).
[19] J. Ries, B. Brezger, and A. I. Lvovsky, Phys. Rev. A **68**, 025801 (2003).
[20] V. Josse, A. Dantan, A. Bramati, M. Pinard, and E. Giacobino, J. Opt. B: Quantum Semiclassical Opt. **5**, S513 (2003).
[21] M. Kauranen, A. L. Gaeta, R. W. Boyd, and G. S. Agarwal, Phys. Rev. A **50**, R929 (1994).
[22] G. S. Agarwal and R. W. Boyd, Phys. Rev. A **38**, 4019 (1988).
[23] A. S. Zibrov and I. Novikova, Zh. Eksp. Teor. Fiz. **82**, 124 (2005);JETP Lett. **82**, 110 (2005).